Biosensors and Bioelectronics 43 (2013) 131–136

Contents lists available at SciVerse ScienceDirect

Biosensors and Bioelectronics

journal homepage: www.elsevier.com/locate/bios

Direct electron transfer glucose biosensor based on glucose oxidase self-assembled on electrochemically reduced carboxyl graphene

Bo Liang [a], Lu Fang [a], Guang Yang [a], Yichuan Hu [a], Xishan Guo [b], Xuesong Ye [a,c,*]

[a] Biosensor National Special Laboratory, Key Laboratory of Biomedical Engineering of Ministry of Education, College of Biomedical Engineering and Instrument Science, Zhejiang University, Hangzhou 310027, PR China
[b] College of Biosystems Engineering and Food Science, Zhejiang University, Hangzhou 310058, PR China
[c] Cyrus Tang Center for Sensor Materials and Applications, Zhejiang University, Hangzhou 310058, PR China

ARTICLE INFO

Article history:
Received 24 September 2012
Received in revised form
19 November 2012
Accepted 29 November 2012
Available online 13 December 2012

Keywords:
Glucose sensor
Carboxyl graphene
Electrochemical reduction
Direct electrochemistry

ABSTRACT

A glucose biosensor based on direct electron transfer of glucose oxidase (GOD) self-assembled on the surface of the electrochemically reduced carboxyl graphene (ERCGr) modified glassy carbon electrode has been reported. X-ray photoelectron spectroscopy (XPS) analyses of ERCGr indicate most of the oxygen-containing groups such as epoxy/ether groups and hydroxyl groups in the carboxyl graphene were eliminated, while carboxylic acid groups remained. GOD was immobilized on the ERCGr modified glassy carbon electrode via self-assembly. The cyclic voltammetric result of the electrode shows a pair of well-defined and quasi-reversible redox peaks with a formal potential of −0.467 V and a peak to peak separation of 49 mV, revealing that the direct electron transfer between GOD and the electrode has been achieved. The proposed biosensor exhibits a linear response to glucose concentrations ranging from 2 to 18 mM with a detection limit of 0.02 mM. Moreover, this facile, fast, environment-friendly and economical preparation strategy of ERCGr may be extended for the preparation of other graphene based enzyme electrode biosensors.

1. Introduction

Diabetes mellitus is a worldwide public health problem and one of the leading causes of death and disability in the world (Pei et al., 2004; Wang, 2008). Since the first initial concept of glucose enzyme electrodes was proposed by Clark and Lyons in 1962 (Clark and Lyons, 1962), tremendous efforts have been made to develop reliable devices for diabetes control. Glucose oxidase (GOD), a flavin enzyme, has been extensively used in glucose sensors. Direct electron transfer between GOD and the electrode surface of glucose biosensors without the assistance of mediators has raised considerable interest over the last three decades in experimental (Guiseppi-Elie et al., 2002; Liu et al., 2005; Shan et al., 2009b; Sheng et al., 2012; Willner et al., 1993) and theoretical (Wang et al., 2010; Yang et al., 2012) researches. The absence of mediators such as ferrocene derivatives, ferricyanide and conducting organic salts etc. is the main advantage of the glucose sensors based on the strategy of direct electron transfer, in which case, the electron is transferred directly from glucose to the electrode via the active site of the enzyme. However, the direct electron transfer for GOD is extremely difficult, since the active site of GOD, flavin adenine dinucleotide (FAD), is deeply embedded within a protective protein shell (Wu and Hu, 2007). Thus, various nanomaterials, such as gold nanoparticles (Qiu et al., 2012; Zhang et al., 2005), carbon nanotubes (Cai and Chen, 2004; Wang and Yao, 2012), graphene (Kang et al., 2009; Wang et al., 2011) and their composites (Chen et al., 2011; Lin et al., 2009; Yang et al., 2008) have been used to promote the electron transfer of redox proteins.

Graphene, a single layer of carbon atoms in a closely packed honeycomb two-dimensional lattice, has attracted considerable attention from both the experimental and theoretical scientific communities in recent years (Geim, 2009; Li and Kaner, 2008). Owing to the excellent electrical, chemical, mechanical and structural properties, such as large surface to volume ratio, high conductivity and electron mobility at room temperature, low energy dynamics of electrons with atomic thickness, robust mechanical properties and flexibility, graphene has stimulated exploding interest in sensor applications (Gan and Hu, 2011; Liu et al., 2012; Shao et al., 2010). Numerous studies report successful achievements of the direct electron transfer of GOD based on graphene (Shan et al., 2009b; Wu et al., 2010; Zhang et al., 2012). However, graphene sheets without functionalization are hydrophobic and easy-to-aggregate in aqueous solution (Gu et al., 2012; Li and Kaner, 2008). Chemical functionalization is generally used to prevent agglomeration, such as long-chain alkylamine (Niyogi et al., 2006), pyrene derivative, 1-pyrenebutyrate (PB-) (Xu et al., 2008), poly-L-lysine (Shan et al., 2009a), 1-pyrenecarboxylic acid

* Corresponding author. Tel.: +86 571 87952756; fax: +86 571 87951676.
E-mail addresses: yexuesong@zju.edu.cn, yexs@mail.bme.zju.edu.cn (X. Ye).

0956-5663/$ - see front matter © 2012 Elsevier B.V. All rights reserved.
http://dx.doi.org/10.1016/j.bios.2012.11.040

(An et al., 2010) and 1-(3-Aminopropyl)-3-methylimidazolium bromide ionic liquid (NH2-IL) (Jiang et al., 2012). However, these methods always need additional chemical reagents and complicated processes.

As we know, carboxyl graphene can form well-dispersed aqueous colloids due to the electrostatic repulsion of these graphene sheets which are negatively charged when dispersed in water as a result of ionization of the carboxylic acid and phenolic hydroxyl groups (Li et al., 2008; Park et al., 2008; Xu et al., 2011). Carboxylic acid groups can react with proteins, carbohydrates or polymers via amide or ester linkages to graft functional molecules (Liu et al., 2012). Huang et al. (2011) presented a biosensor based on carboxylic acid functionalized graphene for the sensitive determination of guanine and adenine. Srivastava et al. (2012) presented a urea sensor by immobilizing urease and glutamate dehydrogenase to carboxylic acid functionalized multilayered graphene via covalent attachment. Furthermore, the amine groups of GOD can be covalently attached to the carboxylic acid groups (Arya et al., 2009; Lin et al., 2004). Liu et al. (2010) has reported a glucose biosensor based on the detection of hydrogen peroxide with GOD covalently attached to the carboxylic acid groups of graphene oxide. However, there are few reports showing that carboxyl graphene has been used for glucose biosensors with direct electron transfer up to now, while the direct electron transfer based biosensor has a lower operating potential and thus has a higher selectivity than those based on the oxidation of hydrogen peroxide (Jiang et al., 2012; Wang, 2008; Wu et al., 2010). The main reason of carboxyl graphene having not been used in direct electron transfer is that the insulating property of carboxyl graphene inhibits the electron transfer of GOD. Moreover, carboxyl graphene is also scarcely reported as conductive media applied for other enzyme electrode biosensors based on direct electron transfer.

In this paper, carboxyl graphene was electrochemically reduced by cyclic voltammetry (Ping et al., 2011; Ramesha and Sampath, 2009). After electrochemical reduction, most of the oxygen-containing groups in the carboxyl graphene were reduced, while carboxylic acid groups remained. The immobilization of GOD was realized via self-assembly under mild conditions. The direct electron transfer between the immobilized GOD and the electrode surface has been achieved efficiently. Compared with other functionalized graphene composite modified glucose biosensors, this sensor shows a comparable electrocatalytic performance, wide linear ranges and high sensitivity but with a facile fabrication approach.

2. Experimental

2.1. Materials

Glucose oxidase (GOD) from *Aspergillus niger*, 1-ethyl-3-(3-dimethylaminoprophy) carbondiimide hydrochloride (EDC), N-hydroxysulfo-succinimide (NHS), ascorbic acid, uric acid, acetaminophen and dopamine were purchased from Aladdin Ltd. (Shanghai, China). Carboxyl graphene (carboxyl ratio 5%) was purchased from Nanjing XFNANO Materials Tech Co., Ltd. (Nanjing, China). All other reagents were purchased from Sinopharm Chemical Reagent Co., Ltd. (Shanghai, China) and were reagent grade. Deionized-ultrafiltered (18 MΩ/cm) water was used for all aqueous solutions. All experiments were carried out in a 0.05 M phosphate-buffered saline (PBS) solution (pH 7.4) unless otherwise specified.

2.2. Apparatus

All electrochemical experiments were performed in an electrochemical workstation (μAutolab III, Metrohm, Switzerland) on a conventional three-electrode system with an Ag/AgCl electrode as the reference electrode, a platinum wire electrode as the counter electrode and a modified glassy carbon electrode as the working electrode. Electrochemical impedance spectroscopy (EIS) measurements were performed in 0.1 M KCl solution containing 5.0 mM $K_3Fe(CN)_6/K_4Fe(CN)_6$ (1:1) with a frequency ranging from 100 kHz to 0.1 Hz. Scanning electron microscopic (SEM) images were collected on a field emission scanning electron microscope (FESEM, SIRION FEI, Netherlands). Samples for SEM were coated with Au films by using a vacuum spin coater. X-ray photoelectron spectroscopy (XPS) analyses were carried out on an ESCALAB MARK II X-ray photoelectron spectrometer (VG Scientific Ltd., UK).

2.3. Preparation of electrodes

The glassy carbon electrode (GCE) with a diameter of 3 mm was successively polished to a mirror shine surface with 0.5 and 0.05 μm alumina powder. After being rinsed with deionized, ultrafiltered water, it was sonicated in ethanol and deionized, ultrafiltered water for 5 min, respectively. The GCE was then dried in nitrogen airflow.

6 μL carboxyl graphene (CGr) water dispersion (2 mg/mL) was cast on the pretreated GCE surface and it is allowed to dry in the ambient condition. The electrochemical reduction of CGr on GCE was performed by cyclic voltammetric scanning from 0.7 to −0.9 V at a scan rate of 0.05 V s^{-1} in N_2-saturated 0.5 M NaCl solution for 5 cycles. After that the electrode was rinsed with 0.05 M PBS thoroughly, and then the electrode was immersed in 0.05 M PBS containing 10 mM EDC and 20 mM NHS for 1 h to activate the carboxylic groups in the electrochemically reduced carboxyl graphene (ERCGr). Then the electrode was washed quickly with PBS and after that it is immediately immersed in a GOD/PBS solution (10 mg/mL GOD, pH 7.4) for 2 h. Afterwards, the electrode (denoted as ERCGr–GOD/GCE) was thoroughly rinsed with deionized, ultrafiltered water, dried in air and stored at 4 °C when not in use.

The same procedure was employed to fabricate ERGO–GOD/GCE in which graphene oxide was used instead of carboxyl graphene. The electrochemical reduction of graphene oxide on GCE was performed by cyclic voltammetric scan as previously described. In comparison with ERCGr–GOD/GCE, CGr/GCE, ERCGr/GCE and CGr–GOD/GCE were prepared by casting CGr on polished GCE, electrochemical reduction of CGr/GCE and self-assembly of GOD on CGr/GCE, respectively. GOD/GCE was prepared by immersing a bare GCE into GOD/PBS solution (10 mg/mL GOD, pH 7.4) for 2 h, which was then rinsed with deionized, ultrafiltered water and dried in air.

3. Results and discussion

3.1. Preparation and characterization of electrodes

Carboxyl graphene (CGr) was electrochemically reduced as described in the above section. Fig. 1A shows the typical cyclic voltammograms (CVs) of electrochemical reduction of CGr with a reduction peak at −0.80 V. However, the peak is only observed at the first cycle, while it is dramatically decreased at the second cycle and disappeared completely after the third cycle. This result is compatible with those in the previous report (Wang et al., 2009). The reduction peak should be attributed to the reduction of oxygen-containing groups on CGr.

The electrochemical reduction result of CGr was investigated by XPS. XPS is a quantitative spectroscopic technique that measures the elemental composition, chemical state and electronic state of the elements that exist within a material, and provides

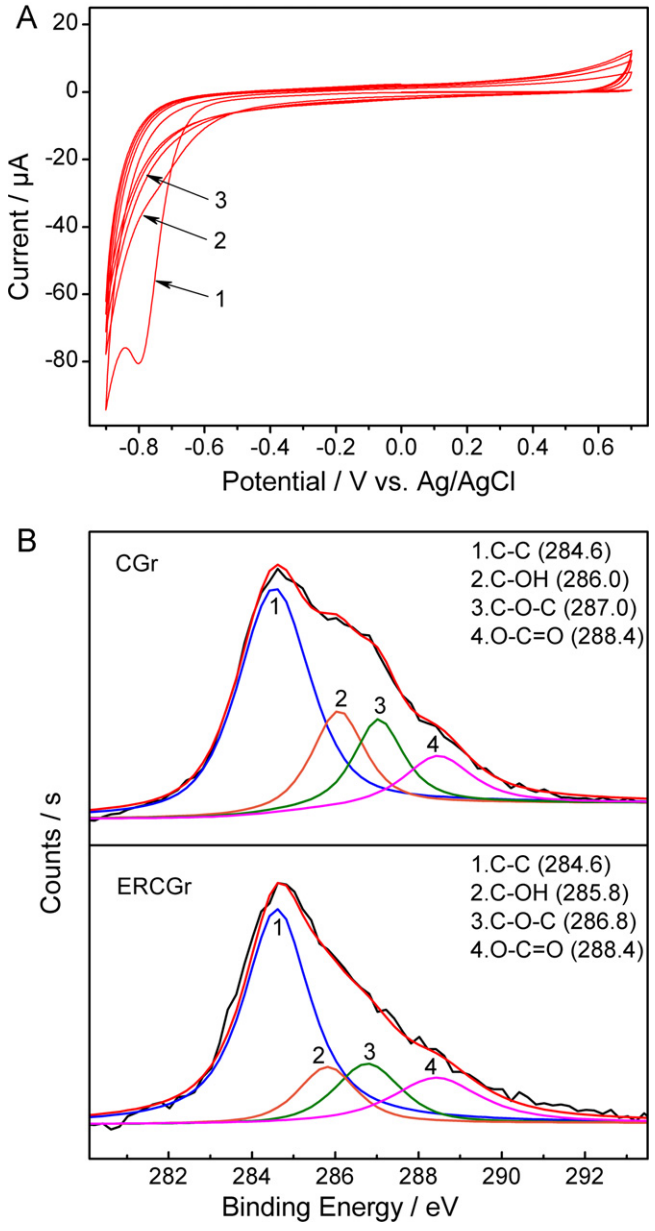

Fig. 1. (A) Cyclic voltammograms of CGr/GCE in N_2-saturated 0.5 M NaCl aqueous solution at a scan rate of 0.05 V s^{-1} and (B) The C1s XPS spectra of CGr and ERCGr.

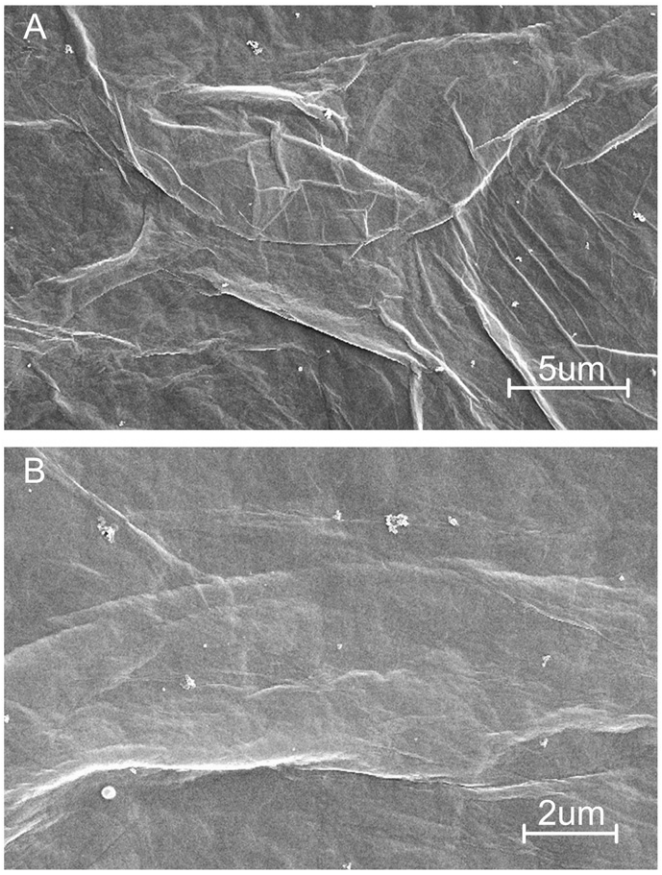

Fig. 2. SEM images of ERCGr (A) and ERCGr–GOD (B).

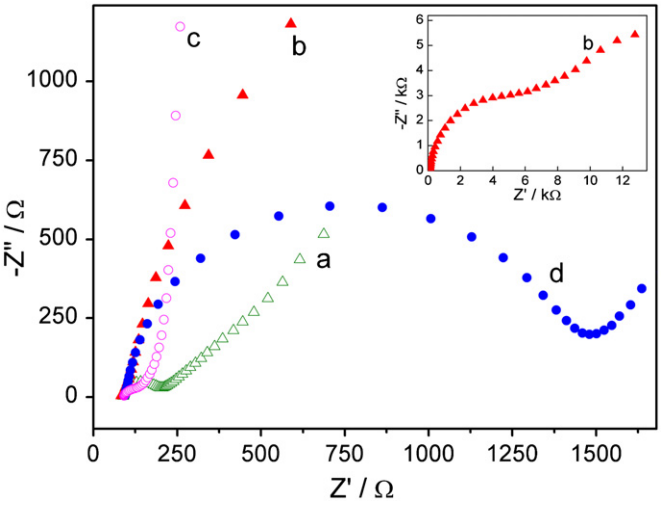

Fig. 3. EIS spectra of bare GCE (a), CGr/GCE (b), ERCGr/GCE (c) and ERCGr–GOD/GCE (d) in 0.1 M KCl aqueous solution containing 5.0 mM $K_3Fe(CN)_6/K_4Fe(CN)_6$. Upper right inset shows full scale of the EIS spectra of CGr/GCE.

the chemical bonding information of the material. Fig. 1B shows the C1s XPS spectra of the CGr and ERCGr. As shown, there are four kinds of carbon atoms in different functional groups, such as ring carbons (C–C) at 284.6 eV, carbons in phenolic hydroxyl groups (C–OH) at 286.0 eV, carbons in epoxy/ether (C–O–C) at 287.0 eV, and carboxylic carbons (O–C═O) at 288.4 eV. The peaks of the C–OH and C–O–C of ERCGr are obviously lower than that of CGr, which indicates that these oxygen-containing groups were reduced during the electrochemical reduction process. However, no evident decrease of the peak area of O–C═O has been observed, suggesting that the carboxylic acid groups remained.

Fig. 2 shows the SEM images of ERCGr and ERCGr–GOD on the surface of GCE. It can be seen that the ERCGr film has a typical crumpled and wrinkled sheet structure of graphene (Fig. 2A), which provides a large rough surface for further immobilization of enzyme. After GOD self-assembly, the ERCGr–GOD formed a homogenous mushy film (Fig. 2B), indicating the successful immobilization of GOD on the surface of the ERCGr modified GCE.

EIS is a powerful technique for studying the interface properties of electrode surfaces. Fig. 3 shows the Nyquist plots of EIS for bare GCE, CGr/GCE, ERCGr/GCE and ERCGr–GOD/GCE. The Nyquist plot of EIS has a semicircle portion at high frequency and a linear portion at low frequency. The semicircle portion corresponds to the charge transfer limited process and the linear portion corresponds to the diffusion process. The charge transfer resistance

(R_{ct}) of the electrode equals to the semicircle diameter. As shown, the R_{ct} of the CGr/GCE (7130 Ω, Fig. 3b) is larger than that of the bare GCE (120 Ω, Fig. 3a), suggesting that a layer of insulative CGr film has formed on the surface of GCE, and hindered the charge transfer from the redox probe of $[Fe(CN)_6]^{3-/4-}$ to the GCE surface. Obviously, the R_{ct} of ERCGr/GCE is dramatically decreasing to 73 Ω (Fig. 3c), which indicates that the conductivity of CGr has been improved by the electrochemical reduction. Moreover, the R_{ct} of ERCGr/GCE is lower than that of the bare GCE, implying that ERCGr formed an interpenetrating network in favor of diffusion of redox probes and interfacial electron transfers. When GOD self-assembled on the surface of ERCGr, the R_{ct} of ERCGr–GOD/GCE increased to 1350 Ω (Fig. 3d), due to the blocking effects of GOD on charge transfer (Yang et al., 2011), which also indicates that GOD has been successfully immobilized.

3.2. Direct electrochemistry of GOD self-assembled on ERCGr/GCE

Direct electrochemistry of GOD self-assembled on ERCGr has been studied by cyclic voltammetry. Fig. 4 shows the CVs of CGr/GCE, CGr–GOD/GCE, ERCGr/GCE and ERCGr–GOD/GCE in N_2-saturated PBS solution (0.05 M, pH 7.4) at a scan rate of 0.10 V s^{-1}. The background current of the ERCGr/GCE (Fig. 4 dash dot line) is higher than that of the CGr/GCE (Fig. 4 dotted line), which is ascribed to the improvement of electrical conductivity by electrochemical reduction of CGr. A pair of well-defined and quasi-reversible redox peaks was observed at the CVs of ERCGr–GOD/GCE (Fig. 4 solid line) with the anodic peak potential (E_{pa}) at −0.442 V and the cathodic peak potential (E_{pc}) at −0.491 V. The peak to peak separation (ΔE_p) is about 49 mV, revealing a fast

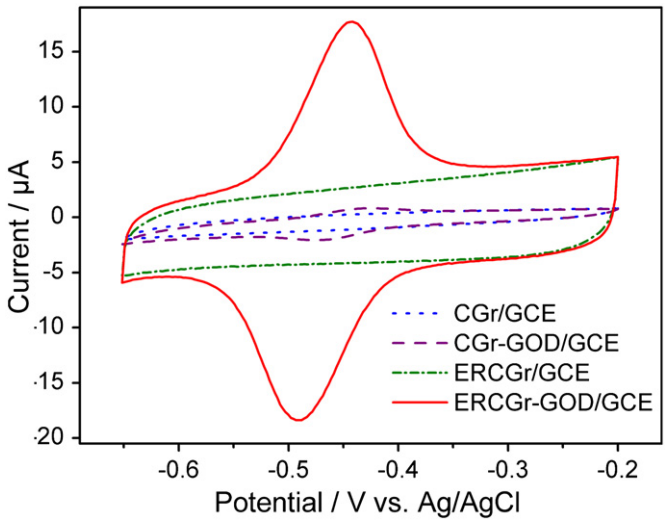

Fig. 4. Cyclic voltammograms of CGr/GCE (dotted line), CGr–GOD/GCE (dashed line), ERCGr/GCE (dash dot line) and ERCGr–GOD/GCE (solid line) in N_2-saturated PBS solution (0.05 M, pH 7.4). Scan rate: 0.1 V s^{-1}.

electron transfer process. The formal potential ($E^{\circ\prime}$) calculated from the average of cathodic and anodic peak potential is −0.467 V, which is close to the electrode potential of GOD in previous reports (Jiang et al., 2012; Kang et al., 2009). From the redox peak characteristics of the ERCGr–GOD/GCE, we could conclude that the direct electron transfer between GOD and GCE has been achieved. In addition, redox peaks at the CVs of CGr–GOD/GCE (Fig. 4 dashed line) can hardly be observed, which is due to the insulating property of carboxyl graphene that inhibits the direct electron transfer between GOD and GCE. Moreover, no redox peaks were observed at the CVs of bare GCE (Fig. S1 dotted line) and GOD/GCE (Fig. S1 dash dot line). This result reveals that the electrochemical reduction of CGr plays a key role in the achievement of direct electron transfer of GOD. The direct electrochemistry of GOD self-assembled on electrochemically reduced graphene oxide (ERGO–GOD/GCE) has also been investigated. A pair of redox peaks was also observed at the CVs of ERGO–GOD/GCE (Fig. S1 dashed line). However, the peak current of the ERGO–GOD/GCE are much lower than that of the ERCGr–GOD/GCE (Fig. S1 solid line). This might be due to that the carboxylic groups in ERGO are less than that in ERCGr, which implies that the carboxylic groups are important for self-assembly of GOD. Moreover, no peaks were observed at the CVs of ERCGr/GCE (Fig. 4 dash dot line). This indicates that the redox peaks of the ERCGr–GOD/GCE should be ascribed only to GOD. All these characteristics reveal that the direct electron transfer between GOD and the electrode has been obtained and promoted by ERCGr modification.

We know that the direct electron transfer of GOD is a two-electron and two-proton coupled reaction as illustrated in Fig. 5. The cathodic peak current (I_{pc}) is attributed to the reduction of GOD(FAD), the oxidized form of GOD, while the anodic peak current (I_{pa}) is attributed to the oxidation of GOD($FADH_2$), the reduced form of GOD. In addition, the ERCGr–GOD/GCE exhibits good electrocatalytic activity toward the reduction of oxygen (O_2) and oxidation of glucose, which will be discussed in the next section.

As the direct electron transfer of GOD is a two-electron and two-proton coupled reaction, the pH value of the solution will influence the direct electron transfer of GOD. Fig. S2 shows the effect of pH on the cyclic voltammetric characteristics of ERCGr–GOD/GCE. Both the anodic and cathodic peak potentials shift to negative direction with the increase of the solution pH. The formal potential ($E^{\circ\prime}$) exhibits a linear dependence on the pH ranging from 5 to 10 with a slope of −51.7 mV/pH (r=0.994), which is close to the theoretical value of −58.6 mV/pH (Liu et al., 2007) for a reversible two-electron and two-proton coupled reaction process, indicating the high reversibility of the direct electron transfer of GOD self-assembled on ERCGr modified GCE.

The influence of the scan rate on the cyclic voltammetric performance of the ERCGr–GOD/GCE was also investigated. Fig. S3 shows the CVs of ERCGr–GOD/GCE in N_2-saturated PBS (0.05 M, pH 7.4) at different scan rates. As shown, the redox peak currents

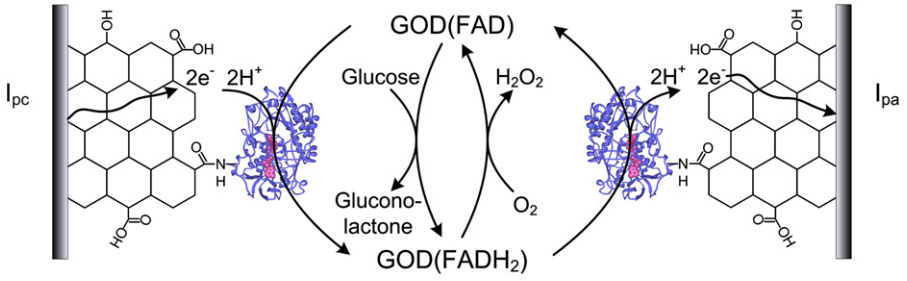

Fig. 5. Scheme of the direct electron transfer of the ERCGr–GOD/GCE and the electrocatalysis of oxygen and glucose.

linearly increased with the scan rates ranging from 20 to 300 mV s^{-1} (Fig. S3 inset). At the same time, the redox potentials (E_{pa} and E_{pc}) of GOD shift slightly. These characteristics indicate that the redox reaction of GOD on the surface of ERCGr/GCE is a quasi-reversible surface-controlled electrochemical process.

3.3. Performance of ERCGr–GOD/GCE based glucose biosensor

The ERCGr–GOD/GCE exhibits good electrocatalytic activity toward the reduction of O_2. Fig. 6A shows CVs of ERCGr–GOD/GCE in PBS (0.05 M, pH 7.4) saturated with N_2 or O_2. A remarkable enhancement of the cathodic peak current was obtained in the presence of O_2, accompanied by a decrease of anodic peak current (Fig. 6A curve b). Furthermore, when glucose was added to the O_2-saturated PBS, the cathodic current decreased (Fig. 6A curve c). CVs of bare GCE and ERCGr/GCE in O_2-saturated PBS (0.05 M, pH 7.4) have also been investigated. Results show that the cathodic peak currents of the bare GCE (Fig. S4 curve b) and the ERCGr/GCE (Fig. S5 curve b) increased in the presence of O_2. However, when glucose was added to the O_2-saturated PBS, no obvious decrease of the cathodic current was observed in both the bare GCE (Fig. S4 curve c) and the ERCGr/GCE (Fig. S5 curve c). This suggests that the enhancement of the cathodic peak current at CVs of ERCGr–GOD/GCE in O_2-saturated PBS is attributed to the GOD catalyzed oxygen reduction. As illustrated in Fig. 5, the reduced form of GOD, GOD($FADH_2$), produced by electrochemical reduction of GOD(FAD), can catalyze the reduction of dissolved oxygen and generate the oxidized form of GOD, GOD(FAD), which can be electrochemically reduced again at the surface of ERCGr/GCE and increase the cathodic current. Furthermore, when glucose is added, the decrease of the cathodic current as shown in Fig. 6A curve c could be attributed to the enzyme-catalyzed glucose oxidation. As illustrated in Fig. 5, the oxidized form of GOD, GOD(FAD), is reduced by glucose, which restrains the electrochemical reduction reaction of GOD(FAD) and decreases the reduction current. This characteristic can be utilized to build a glucose biosensor.

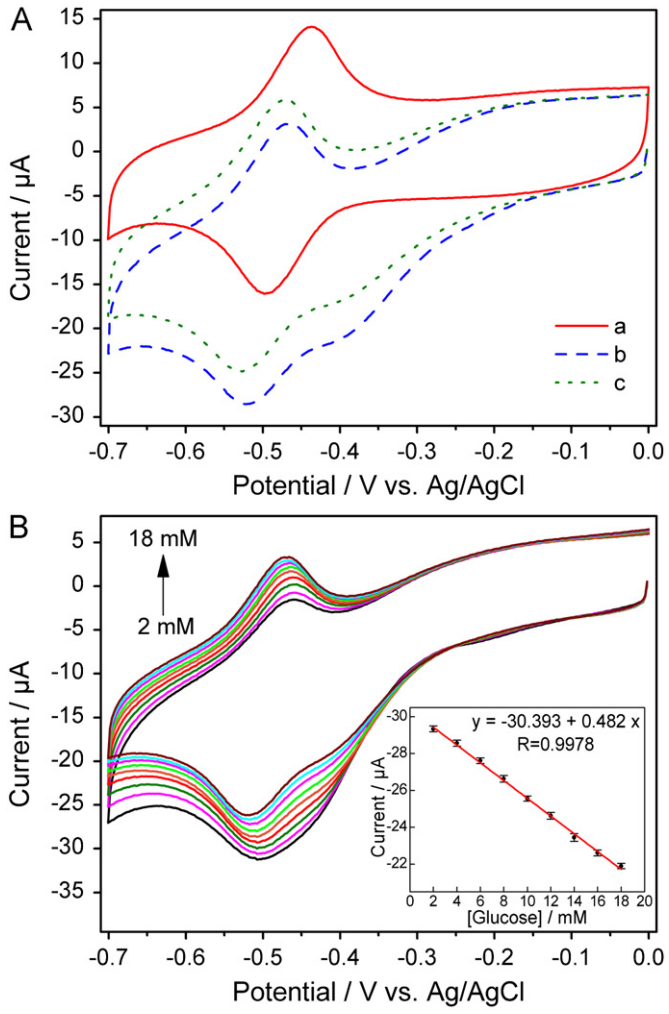

Fig. 6. (A) Cyclic voltammograms of ERCGr–GOD/GCE in N_2-saturated PBS solution (0.05 M, pH 7.4) (a), in O_2-saturated PBS solution (b) and in the O_2-saturated PBS solution after an addition of 10 mM glucose (c); Scan rate: 0.1 V s^{-1}. (B) Cyclic voltammograms of ERCGr–GOD/GCE in the O_2-saturated PBS solution in various concentrations of glucose; Scan rate: 0.1 V s^{-1}. The inset shows the calibration curve of the linear dependence of cathodic peak current on the glucose concentration.

Fig. 6B shows the CVs of ERCGr–GOD/GCE in O_2-saturated PBS (0.05 M, pH 7.4) with different glucose concentrations. As shown, the cathodic peak current decreased linearly with the increase of glucose concentration. The calibration curve corresponding to cyclic voltammetry response is linear against the glucose concentration ranging from 2 to 18 mM with a sensitivity of about 7 μA mM^{-1} cm^{-2} and a correlation coefficient of 0.9978 (Fig. 6B inset). The detection limit is estimated to be 0.02 mM at a signal-to-noise ratio of 3. The linear range of the ERCGr–GOD/GCE is much wider compared to other reported graphene based electrodes, such as 0.5–3.5 mM for GOD on electrochemically reduced graphene oxide and gold-palladium bimetallic nanoparticles modified GCE (Yang et al., 2011), 0.02–6.24 mM for GOD on reduced graphene oxide/zinc oxide composite modified GCE (Palanisamy et al., 2012), 0.08–12 mM for GOD–graphene–chitosan nanocomposite (Kang et al., 2009) and 2–16 mM for GOD on ionic liquid functionalized graphene composite modified GCE (Jiang et al., 2012). The comparison of the analytical performance of the developed electrode with other electrodes reported previously was summarized in Table S1. It can be seen that the ERCGr–GOD/GCE exhibited a wider linear range and an acceptable sensitivity. Moreover, the proposed glucose biosensor was fabricated by a facile and low cost procedure without expensive reagents and complicated experiments. The anti-interference ability of ERCGr–GOD/GCE was achieved by low operating potential rather than interferent diffusion limiting membrane such as nafion or polypyrrole. As is known to us that the normal range of blood glucose concentration is 4.4–6.6 mM (Wang, 2008), and the diabetic glucose concentration is above 7 mM (Dai et al., 2007), so our glucose biosensor is adequate to practical application for detecting blood glucose concentration.

We also investigated the sensor response to glucose in air saturated PBS solutions. Due to the low dissolved oxygen in air saturated PBS solution, the cathodic peak current at CVs of ERCGr–GOD/GCE in air-saturated PBS was lower than that in O_2-saturated PBS, while the anodic peak current was higher than that in O_2-saturated PBS (Fig. S6). As shown in Fig. S6, when glucose was added to the air-saturated PBS, the cathodic current decreased. However, the current response to glucose is lower than that in O_2-saturated PBS and the sensitivity is almost half of that in O_2-saturated PBS.

To evaluate the effect of enzyme loading, we fabricated five electrodes with different GOD concentrations of 1 mg/ml, 5 mg/ml, 10 mg/ml, 15 mg/ml and 20 mg/ml respectively. Fig. S7A shows CVs of the five electrodes in N_2-saturated PBS solution (0.05 M, pH 7.4). With the increase of GOD concentrations, the peak currents enhanced, which indicated more enzymes were immobilized on the electrodes in denser GOD solutions. The EIS of the five electrodes also indicates that more GOD self-assembled to the electrodes with higher GOD concentrations, because the R_{ct} of the electrodes increased with the increasing of the GOD concentrations (Fig. S7B). The effect of enzyme loading on the glucose response was evaluated by the cathodic peak currents change of the CVs of the electrodes in O_2-saturated PBS with 5 mM glucose addition. As shown in Fig. S7C,

the current response increased with GOD concentrations due to the higher enzyme loading in denser GOD solutions. However, when GOD concentrations are more than 10 mg/mL, the increase of the current response became slower. So 10 mg/mL might be the economical GOD concentration.

Selectivity is important in the practical use of biosensors. The compounds such as dopamine (DA), acetaminophen (AP), uric acid (UA) and ascorbic acid (AA) are usually coexisted with glucose in real samples, which may interfere with the determination of glucose. The influence of those interferents was examined by cyclic voltammograms of the electrode with 1 mM DA, AP, UA or AA added to 2 mM glucose solution (O_2-saturated 0.05 M PBS, PH 7.4). As shown in Fig. S8, there were minimal interferences to glucose determination and no additional peaks appeared. The anti-interference ability should be attributed to the low operating potential at which those interferents generate negligible response.

The stability of the biosensor has been investigated. The response current of the modified electrode was reduced by 4.6% of its initial response after two weeks storage at 4 °C in the refrigerator (Fig. S9A). The relative standard deviation (RSD) of the current response to 5 mM glucose was 4% for six measurements, which indicates that the biosensor also has good repeatability (Fig. S9B). To evaluate the reproducibility between different electrodes, five electrodes were fabricated and their responses to 5 mM glucose in O_2 saturated PBS (0.05 M, pH 7.4) were measured under identical conditions. The RSD of the response was 5.4% (Fig. S9C), which indicates that the fabrication method exhibits appreciable reproducibility.

4. Conclusions

In summary, we proposed a glucose biosensor with direct electron transfer based on ERCGr and self-assembly of GOD. XPS results show that the electrochemical reduction of CGr could improve its conductivity by eliminating the oxygen-containing groups such as epoxy/ether groups and hydroxyl groups in CGr, while carboxylic acid groups remained for further immobilization of GOD by self-assembly. The direct electrochemistry of GOD at the modified electrode has been investigated. Cyclic voltammetric result showed a pair of well-defined redox peaks corresponding to the electron transfer of GOD ($FAD/FADH_2$), which indicates that the ERCGr can conduct electron transfer between GOD and the electrode. With the wide linear range, high sensitivity and facile preparation approach for direct electron transfer, this glucose sensor can be used for the detection of diabetic glucose concentrations. Moreover, it will be a useful method to fabricate other analogous enzyme electrode biosensors with direct electron transfer based on carboxyl graphene.

Acknowledgments

This work was financially supported by the National Key Technology R&D Program of China (No. 2012BAI16B02), the National Natural Science Foundation of China (Nos. 60875078, 81171416) and the Nature Science Foundation of Zhejiang Province of China under Grant Z1080300.

Appendix A. Supporting information

Supplementary data associated with this article can be found in the online version at http://dx.doi.org/10.1016/j.bios.2012.11.040.

References

An, X., Simmons, T., Shah, R., Wolfe, C., Lewis, K.M., Washington, M., Nayak, S.K., Talapatra, S., Kar, S., 2010. Nano Letters 10, 4295–4301.
Arya, S.K., Solanki, P.R., Datta, M., Malhotra, B.D., 2009. Biosensors & Bioelectronics 24, 2810–2817.
Cai, C.X., Chen, J., 2004. Analytical Biochemistry 332, 75–83.
Chen, Y., Li, Y., Sun, D., Tian, D.B., Zhang, J.R., Zhu, J.J., 2011. Journal of Materials Chemistry 21, 7604–7611.
Clark Jr., L.C., Lyons, C., 1962. Annals of the New York Academy of Sciences 102, 29–45.
Dai, Z., Ni, J., Huang, X., Lu, G., Bao, J., 2007. Bioelectrochemistry 70, 250–256.
Gan, T., Hu, S.S., 2011. Microchimica Acta 175, 1–19.
Geim, A.K., 2009. Science 324, 1530–1534.
Gu, H., Yu, Y.Y., Liu, X.Q., Ni, B., Zhou, T.S., Shi, G.Y., 2012. Biosensors & Bioelectronics 32, 118–126.
Guiseppi-Elie, A., Lei, C.H., Baughman, R.H., 2002. Nanotechnology 13, 559–564.
Huang, K.J., Niu, D.J., Sun, J.Y., Han, C.H., Wu, Z.W., Li, Y.L., Xiong, X.Q., 2011. Colloids and Surfaces B 82, 543–549.
Jiang, Y.Y., Zhang, Q.X., Li, F.H., Niu, L., 2012. Sensors and Actuators B-Chemical 161, 728–733.
Kang, X.H., Wang, J., Wu, H., Aksay, I.A., Liu, J., Lin, Y.H., 2009. Biosensors & Bioelectronics 25, 901–905.
Li, D., Kaner, R.B., 2008. Science 320, 1170–1171.
Li, D., Müller, M.B., Gilje, S., Kaner, R.B., Wallace, G.G., 2008. Nature Nanotechnology 3, 101–105.
Lin, J.H., He, C.Y., Zhao, Y., Zhang, S.S., 2009. Sensors and Actuators B-Chemical 137, 768–773.
Lin, Y.H., Lu, F., Tu, Y., Ren, Z.F., 2004. Nano Letters 4, 191–195.
Liu, Q., Lu, X., Li, J., Yao, X., 2007. Biosensors & Bioelectronics 22, 3203–3209.
Liu, Y., Wang, M.K., Zhao, F., Xu, Z.A., Dong, S.J., 2005. Biosensors & Bioelectronics 21, 984–988.
Liu, Y., Yu, D.S., Zeng, C., Miao, Z.C., Dai, L.M., 2010. Langmuir 26, 6158–6160.
Liu, Y.X., Dong, X.C., Chen, P., 2012. Chemical Society Reviews 41, 2283–2307.
Niyogi, S., Bekyarova, E., Itkis, M.E., McWilliams, J.L., Hamon, M.A., Haddon, R.C., 2006. Journal of the American Chemical Society 128, 7720–7721.
Palanisamy, S., Vilian, A.T.E., Chen, S.M., 2012. International Journal of Electrochemical Science 7, 2153–2163.
Park, S., An, J., Piner, R.D., Jung, I., Yang, D., Velamakanni, A., Nguyen, S.B.T., Ruoff, R.S., 2008. Chemistry of Materials 20, 6592–6594.
Pei, J., Tian, F., Thundat, T., 2004. Analytical Chemistry 76, 292–297.
Ping, J.F., Wang, Y.X., Fan, K., Wu, J., Ying, Y.B., 2011. Biosensors & Bioelectronics 28, 204–209.
Qiu, C.C., Wang, X., Liu, X.Y., Hou, S.F., Ma, H.Y., 2012. Electrochimica Acta 67, 140–146.
Ramesha, G.K., Sampath, S., 2009. Journal of Physical Chemistry C 113, 7985–7989.
Shan, C., Yang, H., Han, D., Zhang, Q., Ivaska, A., Niu, L., 2009a. Langmuir 25, 12030–12033.
Shan, C.S., Yang, H.F., Song, J.F., Han, D.X., Ivaska, A., Niu, L., 2009b. Analytical Chemistry 81, 2378–2382.
Shao, Y.Y., Wang, J., Wu, H., Liu, J., Aksay, I.A., Lin, Y.H., 2010. Electroanalysis 22, 1027–1036.
Sheng, Q., Liu, R., Zheng, J., Lin, W., Li, Y., 2012. Journal of Solid State Electrochemistry 16, 739–745.
Srivastava, R.K., Srivastava, S., Narayanan, T.N., Mahlotra, B.D., Vajtai, R., Ajayan, P.M., Srivastava, A., 2012. ACS Nano 6, 168–175.
Wang, J., 2008. Chemical Reviews 108, 814–825.
Wang, K., Liu, Q., Guan, Q.M., Wu, J., Li, H.N., Yan, J.J., 2011. Biosensors & Bioelectronics 26, 2252–2257.
Wang, Q.A., Xu, W., Wu, P., Zhang, H., Cai, C.X., Zhao, B., 2010. Journal of Physical Chemistry B 114, 12754–12764.
Wang, Y., Yao, Y.J., 2012. Microchimica Acta 176, 271–277.
Wang, Z.J., Zhou, X.Z., Zhang, J., Boey, F., Zhang, H., 2009. Journal of Physical Chemistry C 113, 14071–14075.
Willner, I., Riklin, A., Shoham, B., Rivenzon, D., Katz, E., 1993. Advanced Materials 5, 912–915.
Wu, P., Shao, Q.A., Hu, Y.J., Jin, J.A., Yin, Y.J., Zhang, H., Cai, C.X., 2010. Electrochimica Acta 55, 8606–8614.
Wu, Y., Hu, S., 2007. Microchimica Acta 159, 1–17.
Xu, C.H., Wang, J.C., Wan, L., Lin, J.J., Wang, X.B., 2011. Journal of Materials Chemistry 21, 10463–10471.
Xu, Y., Bai, H., Lu, G., Li, C., Shi, G., 2008. Journal of the American Chemical Society 130, 5856–5857.
Yang, G., Kang, Z., Ye, X., Wu, T., Zhu, Q., 2012. Biomaterials 33, 8757–8770.
Yang, J., Deng, S.Y., Lei, J.P., Ju, H.X., Gunasekaran, S., 2011. Biosensors & Bioelectronics 29, 159–166.
Yang, J., Zhang, R.Y., Xu, Y., He, P.G., Fang, Y.Z., 2008. Electrochemistry Communications 10, 1889–1892.
Zhang, S.X., Wang, N., Yu, H.J., Niu, Y.M., Sun, C.Q., 2005. Bioelectrochemistry 67, 15–22.
Zhang, Y.Q., Fan, Y.J., Wang, S.S., Tan, Y.L., Shen, X.C., Shi, Z.J., 2012. Chinese Journal of Chemistry 30, 1163–1167.